

Kinetics of TSCD zinc oxide nano-layer growth by modified diffuse-interface model

S.K. Sadrnezhad, M.R. Vaezi*

Center of Excellence for Advanced Processes of Production and Shaping of Materials, Department of Materials Science and Engineering, Sharif University of Technology, Tehran, Iran

Received 20 October 2005; received in revised form 11 November 2005; accepted 20 April 2006

Available online 12 September 2006

Abstract

Deposition of zinc oxide films from aqueous solutions containing complex Zn^{2+} ions on soda-lime substrates were studied by two-stage chemical deposition (TSCD) process. It was shown that the film thickness can be controlled by the number of dipping stages. Nano-layers were produced with less than nine times dipping stages. Greater dipping numbers resulted in film thickness exceeding 100 nm. The growth rate obeyed double-stage zeroth order with respect to the concentration and first order with respect to the temperature. This rate was proportional to the difference between the temperature of the hot water and the substrate. Overall activation energy of $17.20 \pm 0.42 \text{ kJ mol}^{-1}$ and frequency factor of $2.81 \pm 0.07 \mu\text{m s}^{-1}$ was determined for ZnO deposition. These values were attributed to two resistances. One resistance corresponded with film heat transfer mechanism. The other was attributed to species attachment to the solid substrate. A modification to the diffuse-interface kinetic model was devised for explanation of the latter. EDAX (electron dispersive elemental analysis), XRD (X-ray diffraction) and SEM (scanning electron microscopy) were used to characterize the layer formed. These methods showed that the product consisted solely of pure elliptical ZnO grains. © 2006 Elsevier Ltd and Techna Group S.r.l. All rights reserved.

Keywords: Nano-film; Zinc oxide; Thin layer; Kinetics; Heat transfer; TSCD; Diffuse-interface

1. Introduction

Industrial emissions plus urban traffic rise have caused continued environmental pollution growth. Reliable sensing device is needed to monitor the process [1]. The use of sensors has, thus, been increasingly grown at an astounding rate in the last few decades for detection of smoke, hazardous gases, dust and humidity [2–4]. Semi-conducting metal oxides of high gas absorption capability such as ZnO, SnO₂, TiO₂ and WO₃ have been used to detect the environmental polluting species [5]. Particulates present in the off-gases from coal burning and pyrometallurgical systems usually absorb the evolved sulfur bearing gases [6]. The possibility of chemisorption of the sulfur dioxide molecules on metallic oxide has been studied by heating submicron ZnO powders with SO₂ in horizontal tube furnaces before [6].

A film with high electrical conductivity is more desirable for gas sensing purposes. Nano-layers with thicknesses lower than 100 nm are preferred because of their relatively low electrical resistivity [7]. Production of gas sensing nano-films has recently been studied by numerous authors [8,9]. ZnO nano-layers have for example been produced by metallorganic chemical vapor deposition (MOCVD) [10], pulsed laser deposition (PLD) [11], sputtering [12], electron beam evaporation [12], spray pyrolysis [13]. No information is, however, available on nano-film ZnO crystallites deposition by TSCD process investigated in this research.

Keen attention has recently been paid to ZnO and SnO₂ because of their high sensitivity to the polluting materials at low temperatures [14]. Determination of the sensing properties of a material is based on measurement of its resistance (or conductance) when they change due to the contacting of the material with a target gas [15]. Two-stage chemical deposition (TSCD) is a promising method for production of a thin detecting layer applicable to pollution species because of its simplicity and economical feasibility [7]. This method is used in this research for production of ZnO films. The substrate was first immersed into a cold aqueous solution containing a

* Corresponding author. Fax: +98 21 66005717.

E-mail addresses: sadrnezh@sharif.edu (S.K. Sadrnezhad), vaezi9016@yahoo.com (M.R. Vaezi).

complex compound consisting of Zn^{2+} ions. The substrate was covered with a layer of the complex. It was then dipped into a distilled boiling water bath to facilitate the decomposition of the complex compound into the desirable ZnO layer [16]. The layer had a relatively low electrical conductivity that could be improved by doping with SnCl_2 or by annealing [17].

Decomposition reaction could produce new phases comprising of solid, liquid and gas. The ease with which the produced molecules were attached to the growing interface was related to the structure of the interface. Two types of structures could be considered [18]:

- Ordering of the atoms gradually increasing within the interface towards the fully crystalline side until essentially all the atoms were in their appropriate lattice sites.
- Transition from fluid medium to the solid taking place over a number of atomic layers that comprised a diffuse-interface.

The first type of the growth could produce a flat interface associated with close-packed structure of the molecules. This type of interface did not attribute to the layers produced in this research. It looked most appropriate for vapor deposition processes usually occurring on solid surfaces [18]. The second type of the interface was, however, most appropriately attributed to the deposition processes occurring in this research.

The rate of thickening of the oxide film on the substrate was related to the difference between hot water temperature and substrate surface covering complex (ΔT). Measurements showed that the growth rate of the layer depends on both time and temperature. The activation energies and the frequency factors of the process were obtained from the empirical information. The first Newton law for convection transfer was combined with the diffuse-interface kinetic model to quantify the information obtained from the experiments.

2. Experimental procedure

Soda-lime flat (25 mm × 15 mm × 1 mm) and spherical ($\text{Ø}14.5$ mm) glass substrates were used as solid substrates for thin film growth. After degreasing, the substrates were washed with deionized water and dried in a stream of hot air. Aqueous solutions containing $(\text{NH}_4)_2\text{ZnO}_2$ were prepared by mixing

concentrated NH_4OH with 100 cm^3 of 0.5 M ZnCl_2 until white $\text{Zn}(\text{OH})_2$ was precipitated. Further addition of NH_4OH resulted in dissolving of the precipitate. The solution was diluted up to 0.1 M concentration of Zn^{2+} complex. This was found to be the most convenient concentration for production of a good quality film on the substrate. The cleaned glass substrate was first immersed into a complex-containing solution having a temperature between -15 and $+15$ °C and then in a hot water (90 to 105 °C) for 1–15 s.

Nitrogen was bubbled into the liquid by a plastic tube from different locations to create different flow patterns around the substrates. Gas flow rate was changed from 4000 to 16,000 cm^3/min . At 95 °C, effect of flow of gas on the rate of growth of the nano- and thin layer was measured.

Crystalline structure of the film was determined by X-ray diffraction (XRD) method. XRD diffractograms were obtained using $\text{Cu K}\alpha$ radiation beams produced by a Philips PW1390 apparatus. Knowing the surface area of the substrate and the deposited mass of the layer, the thickness of the film was determined by assuming the density of the precipitate to be 5.606 g cm^{-3} [19]. Thickness measurements made by scanning electron microscopy of the samples gave similar results. SEM was also used to study the growth mechanism and the surface morphology of the thin grown layer. Semi-quantitative analyses of the grown layers were determined with a Kevex model EDAX system. Varian-AA6 atomic absorption equipment determined the composition and Hana pH probe measured pH of the solution at different deposition temperatures.

3. Results and discussion

The thickness of the layer increases with the number of dipping stages. Variation of thickness of the deposited film is plotted against the number of dipping stages in Fig. 1. Thicknesses in the nano-range is only produced with the dipping numbers lower than 10. Fig. 2 depicts the SEM cross sectional image of an oxide film after 100 times of dipping. The formation of the oxide layer via TSCD method involves the following pseudo-decomposition reaction:

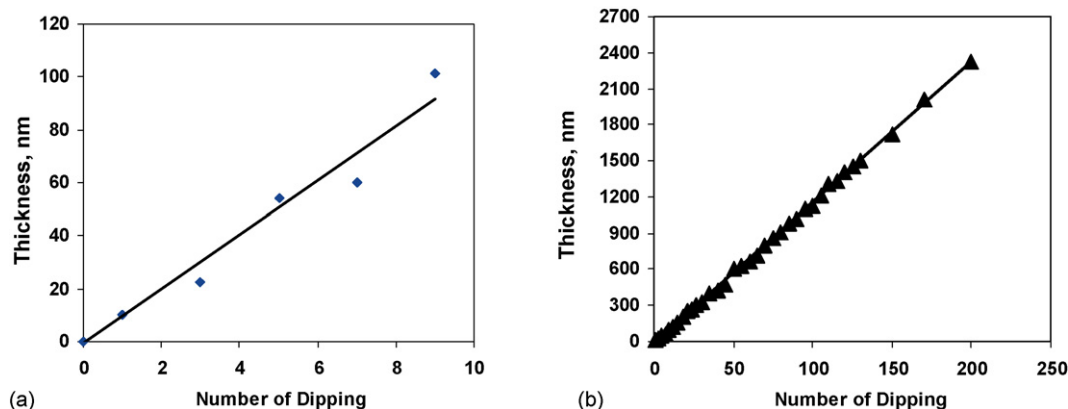


Fig. 1. Thickness of the deposited film vs. the number of dipping stages (a) nano-size and (b) 0–2.4 μm .

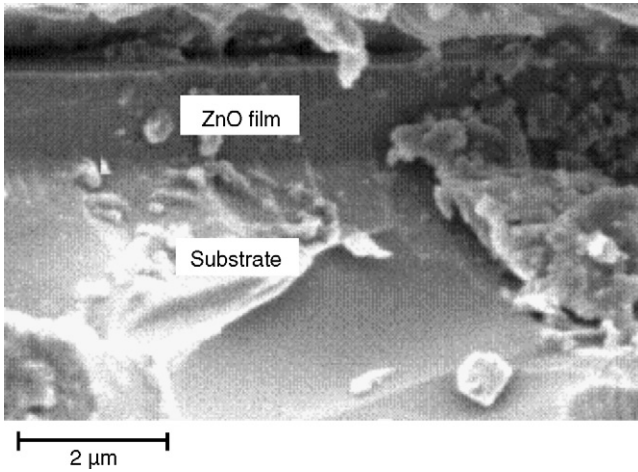


Fig. 2. SEM cross sectional image of the oxide film formed after 100 times dipping of the specimen into the aqueous solution.

The rate of this reaction is experimentally proved independent of the concentration of the $(\text{NH}_4)_2\text{ZnO}_2$ complex. Growth rate of the ZnO layer depends on the hot water temperature. Its slope gradually reduces with the holding time inside the water. It is proportional to the difference between the temperature of the hot water and the $(\text{NH}_4)_2\text{ZnO}_2$ complex.

3.1. Kinetics of oxide deposition

ZnO growth can be composed of the following general steps:

- Decomposition of the complex species to form solid, liquid and gas molecules specified with Eq. (1).
- Outwards transfer of the products from the reaction front.
- Joining of ZnO molecules to the thin film or glass substrate to thicken the covering layer.

Changing complex concentration and measuring the thickness of the thin layer against time at various temperatures clearly indicates a zeroth order growth rate with respect to concentration (Fig. 3). Experimentally determined rates prove the approximate independence of the ZnO growth rate from reactant concentration. Effect of concentration on the film growth rate is therefore ignorable

$$-\frac{dC}{dt} = kC^n, \quad n = 0 \quad (2)$$

C is the molar concentration of the complex, t is the time after immersion and n is the order of the reaction, being zero in this case.

Experimental investigations show that the rate of growth of the ZnO is proportional to the difference between the temperature of the hot water and the $(\text{NH}_4)_2\text{ZnO}_2$ complex, ΔT_1 (Fig. 4). Its slope gradually decreases with submersion time. This seems to be due to the gradual increasing of the complex temperature as a result of rising of the substrate temperature. An external heat transfer model can thus be used

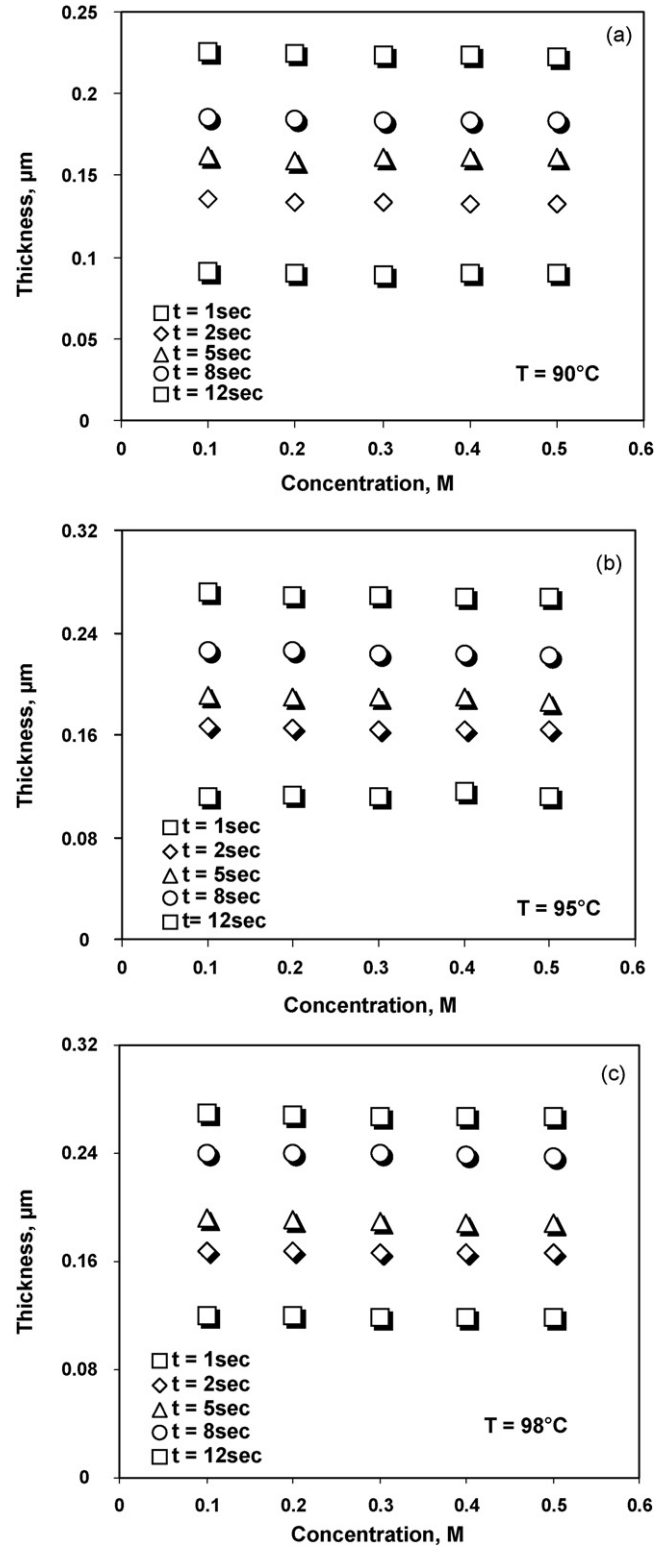


Fig. 3. Effect of concentration on thickness of ZnO layer measured at different times and temperatures.

to explain the film growth rate

$$\frac{d\delta}{dt} = \frac{\dot{q}}{\Delta H_{G\rho}} M_{\text{ZnO}} = \frac{h\Delta T_1}{\Delta H_{G\rho}} M_{\text{ZnO}} \quad (3)$$

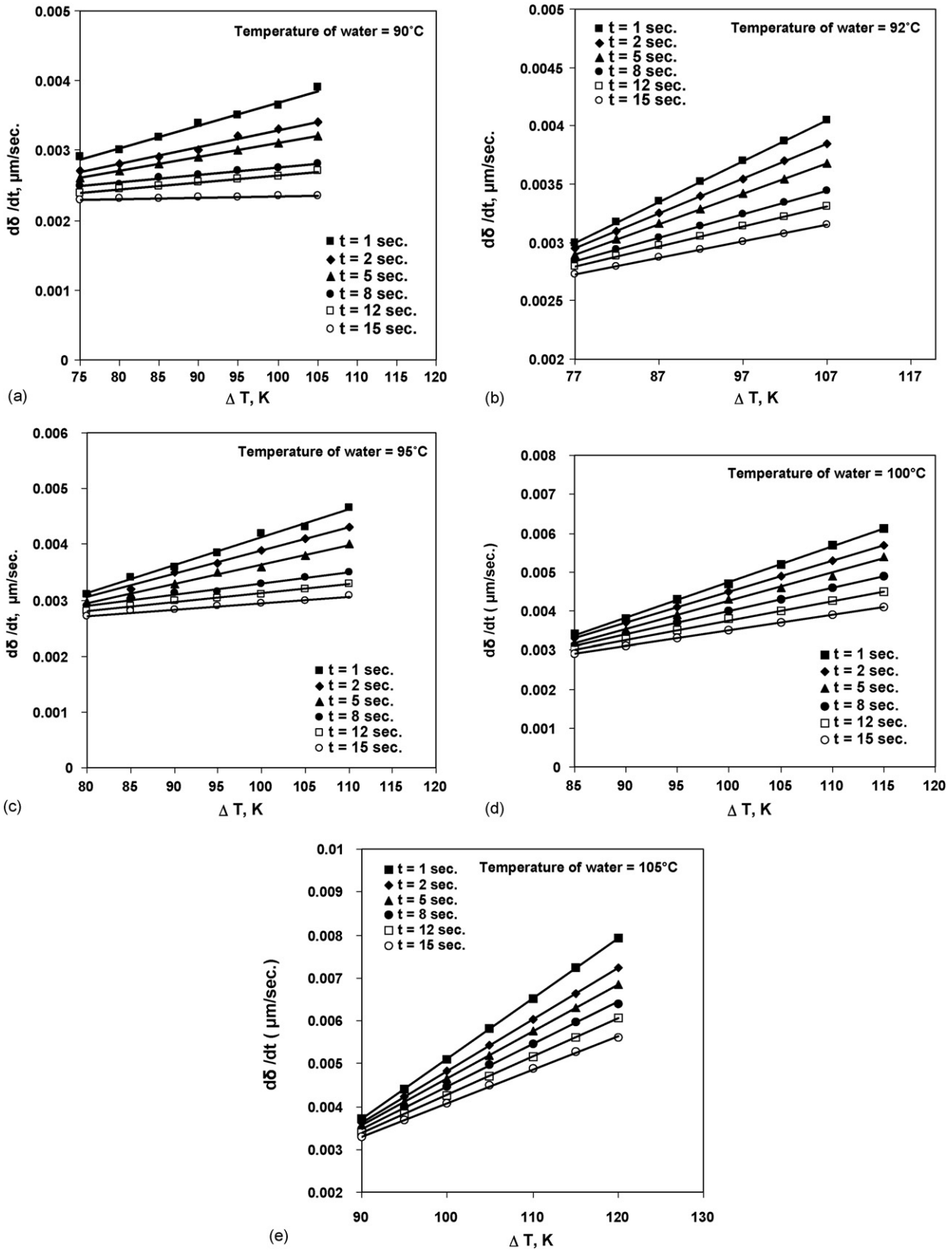


Fig. 4. Effect of the difference between the temperature of the hot water and the complex, ΔT_1 , on the rate of growth of the thickness of the ZnO layer at hot water temperatures of (a) 90 °C, (b) 92 °C, (c) 95 °C, (d) 100 °C and (e) 105 °C.

where δ is the film thickness, \dot{q} is the heat flux, ΔH_G is the enthalpy of the reaction, ρ is the density of the solid layer, M_{ZnO} is the molar weight of ZnO and h is the heat transfer coefficient from hot water to the complex layer attached to the substrate. The heat transfer coefficient h depends on the mean temperature of the reactants defined by the following equation:

$$T = \frac{T_{H_2O}M_{H_2O} + T_{complex}M_{complex}}{M_{H_2O} + M_{complex}} \quad (4)$$

Effect of liquid stirring on the thickness of the ZnO layer is illustrated in Fig. 5. Because of the stirred nature of the dipping process, the second step (b) is fast enough to be ignored in our evaluation rate. Experimental results approved this effect. Stirring of the liquid with different speeds and at different directions shows a negligible effect on the thickness–time curves. Fig. 5 indicates, for example, that variation of the rate of growth of the ZnO thin layer due to the N₂ bubbling at different positions inside the reaction vessel is lower than 5%, which can be considered insignificant. The first and the third kinetic steps may thus be considered as the two influencing rate-controlling steps.

The coefficient of the rate equation is composed of two independent terms. The first term is related to the Newton law of convection, as illustrated by Eq. (3). The second term is related to the diffuse-interface kinetic model [18] for attachment of the ZnO molecules to the solid substrate. From morphological investigation of the oxide layer, it was found that the interface was at least several layers thick. From the liquid–solid nature of the interface and the decomposition characteristics of the reaction that originated the formation of the solid phase, it was concluded that the interface could not be microscopically flat. The classical laws related to the microscopically flat interfaces could, however, be extended with little difficulty to the slightly diffuse-interfaces expected in liquid–solid transitions that could result in this thin layer deposition process. Diffuse-interfaces could generally grow much easier than the flat ones.

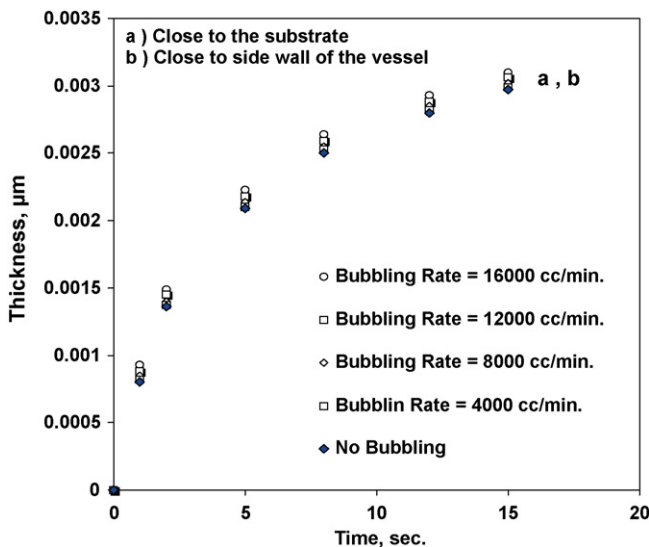


Fig. 5. Effect of liquid stirring on the thickness of the ZnO layer.

We tried, therefore, to investigate this phenomenon with a simple quasi-chemical model in line with the ideas generally developed for a vapor deposition process. To perform this treatment, let us imagine an ideally close-packed flat interface, except that there is an indentation in a step present at the interface. If an ion deposits on the solid at a point on the close-packed flat face, it would join to the three nearest neighbors. If it deposits at a jog, it has three nearest neighbors below the closed-packed plane and three other nearest neighbors on its own plane. The driving force for deposition of the ion at the jog is hence twice that at the position on the close-packed face. This indicates that any ion depositing at a point on the close-packed face can lower its energy further by migrating towards and depositing at a jogged position. Jogs help the deposition and the solid layer grows further. This phenomenon seems especially interesting because of high concentration of jogs present on an ideally diffuse-interface layer [18].

Kinetics of growth of the solid phase can simply be determined in terms of the classical theoretical rate. The frequency ω_1 with which molecules (composed of positive and negative ions) would pass from the complex containing solution to the oxide layer is exponentially related to the temperature

$$\omega_1 = \omega_0 \exp\left(\frac{-Q_1}{RT}\right) \quad (5)$$

ω_0 is the frequency of vibration of the molecules and Q_1 is the activation energy for transport of the molecules from the solution to the oxide layer. Solid molecules will similarly jump in the reverse direction, from oxide layer to the solution. The reverse frequency of molecules, ω_2 , can similarly be given by

$$\omega_2 = \omega_0 \exp\left(\frac{-Q_2}{RT}\right) \quad (6)$$

where Q_2 is the activation energy of molecules transferring from the oxide layer to the solution. The net jumping frequency of the molecules across the interface, ω_G , can thus be determined from the difference between the forward and backward transport frequencies of the molecules as follows:

$$\omega_G = \omega_1 - \omega_2 = \omega_0 \left[\exp\left(\frac{-Q_1}{RT}\right) - \exp\left(\frac{-Q_2}{RT}\right) \right] \quad (7)$$

Substituting $\Delta G_G = Q_1 - Q_2$ in Eq. (7), we find

$$\omega_G = \omega_0 \exp\left(\frac{-Q_1}{RT}\right) \left[l - \exp\left(\frac{\Delta G_G}{RT}\right) \right] \quad (8)$$

From general thermodynamics relationships, we also have

$$\Delta G_G = \Delta H_G - T\Delta S_G \cong \Delta H_G - T \frac{\Delta H_G}{T_{DP}} = \Delta H_G \frac{\Delta T_2}{T_{DP}} \quad (9)$$

in which ΔG_G , ΔH_G and ΔS_G are changes of free energy, enthalpy and entropy of the deposition process, respectively and ΔT_2 is the difference between the zinc containing complex and solid substrate. T_{DP} is referred to the equilibrium deposition temperature, which is a constant value and can be experimentally measured. Substituting Eq. (8) into Eq. (9) and assuming that the exponent is small, the following relationship is

obtained:

$$\omega_G = \omega_1 \left[1 - \exp\left(\frac{\Delta H_G \Delta T_2}{RT_{DP}^2}\right) \right] \quad (10)$$

Assuming all sites on the interface are favorable for growth, the rate of continuous growth V_G is equal to $d_m \omega_G$, where d_m is the distance that the interface advances when a molecule is added into it. Hence

$$V_G = d_m \omega_1 \left[1 - \exp\left(\frac{\Delta H_G \Delta T_2}{RT_{DP}^2}\right) \right] \quad (11)$$

The dependence of the jumping frequency to the diffusion coefficient of the molecule is given by

$$\omega = \frac{6D}{d_m^2} \quad (12)$$

The frequency with which each atom strikes the solution, film interface is usually taken to be one-sixth of its jumping frequency in the bulk solution. Therefore, we have

$$\omega_1 = \frac{D_1}{d_m^2} \quad (13)$$

where D_1 is the mean diffusion coefficient of the depositing species into the oxide layer.

Substitution of Eq. (13) into (11) yields

$$V_G = \frac{D_1}{d_m} \left[1 - \exp\left(\frac{\Delta H_G \Delta T_2}{RT_{DP}^2}\right) \right] \quad (14)$$

Eq. (14), termed the Sadrnezhad–Vaezi equation gives the growth rate of the thin film produced by TSCD method on the soda-lime substrate. According to this equation, a greater difference between the complex and the substrate temperatures results in a greater growth rate. This phenomenon is, however, limited to the decomposition conditions at the reactants position. In order to determine the equilibrium deposition temperature, variations with temperature of both pH and weight of the deposited complex were determined and plotted against temperature, as shown in Fig. 6. Concomitant blank tests were also performed in order to determine the general decomposition effects. Both samples were submerged horizontally into the corresponding solutions so that the partial pressures of the gases could remain invariable. At temperatures about 10 °C, the general complex decomposition resulted in very slow changes in the pH reduction as well as the weight gain (Fig. 6). Careful examinations indicated that the equilibrium decomposition temperature is equal to 10 ± 2 °C. Complex decomposition process continued above this temperature. Changes of the temperature could, therefore, affect on both ΔG_G and pH values of the system.

Total conversion time of the process can be determined by addition of the times obtained from conversion heat transfer and molecular deposition process. The result can lead us to the following rate equation:

$$\frac{d\delta}{dt} = \frac{\Delta T}{(\Delta H_G \rho / h) + (d_m R T_{DP}^2 / D_1 \Delta H_G)} = U \Delta T \quad (15)$$

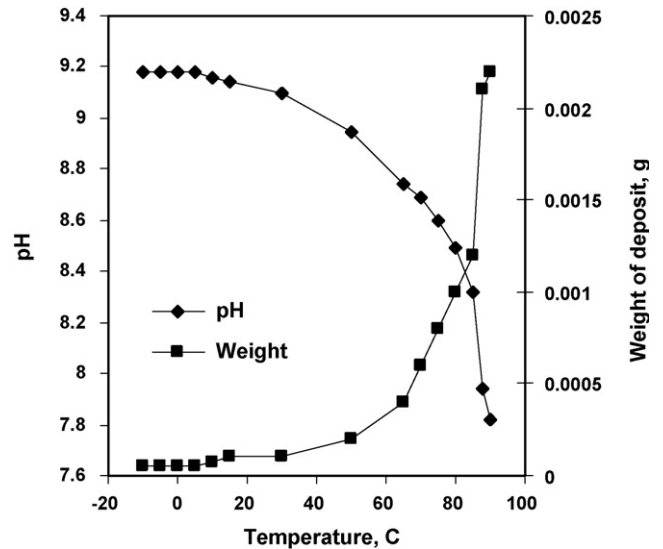


Fig. 6. Effect of temperature on weight of deposit and pH of the solution.

where U is an overall growth-rate constant for the film deposition and ΔT is the difference between the temperature of the hot water and the substrate. Table 1 gives the values of U obtained at different times and temperatures. Arrhenius law calculations (Eq. (16)) yields an overall activation energy and frequency factor for the whole process

$$U = U_0 \exp\left(-\frac{Q}{RT}\right) \quad (16)$$

The results are as follows:

$$Q = 17.20 \pm 0.42 \text{ kJ mol}^{-1} \quad (17)$$

$$U_0 = 2.81 \pm 0.07 \mu\text{m s}^{-1} \quad (18)$$

These values are within the ranges of the external heat and mass transfer processes investigated by previous authors [20–22] indicating the consistency of the results obtained in this research with those available in the literature.

3.2. Film characterization

Scanning electron microscope images of the surface of the oxide layers produced after 100 times immersion into hot water are illustrated in Fig. 7. Morphologies shown in the figure indicate that the ZnO coverage increases with the water temperature.

Based on EDAX elemental analysis, XRD diffractogram and SEM tests, the deposited layers turned out to consist solely of crystalline ZnO grains. EDAX spectrum of the ZnO film shows the presence of Zn, O, Ca, Si and a trace amount of Cl (Fig. 8). The source of Si is the substrate. Ca may have come either as an impurity with the raw materials or may be from the substrate. The Cl species may have come from the aqueous complex solution. Atomic absorption spectroscopy (AAS) has approved these expectations. AAS analysis showed, for example, 76.4 wt.% Zn in the sample produced by 100 times dipping process. EDAX elemental analysis indicated 78.2 wt.% Zn.

Table 1

Overall growth rate constant, U , for the film deposition process calculated from the experimental data for different temperatures and times

Temperature of hot water (°C)	U ($\mu\text{m}/(\text{K s})$)					
	$t = 1 \text{ s}$	$t = 2 \text{ s}$	$t = 5 \text{ s}$	$t = 8 \text{ s}$	$t = 12 \text{ s}$	$t = 15 \text{ s}$
90	0.000030	0.000025	0.000020	0.000015	0.000010	0.000002
92	0.000040	0.000035	0.000030	0.000026	0.000020	0.000010
95	0.000050	0.000040	0.000030	0.000027	0.000020	0.000010
100	0.000090	0.000080	0.000070	0.000060	0.000050	0.000040
105	0.00019	0.00017	0.00015	0.00012	0.000090	0.000080

The difference seems within the acceptable range of errors possibly existing in our experiments.

Fig. 9 shows XRD spectrum of zinc oxide layer produced after 40 trials of the dipping–growing process. The peaks

appearing at $2\theta = 31.3$, 34.6 , and 36.2 correspond to $(1\ 0\ 0)$, $(0\ 0\ 2)$ and $(1\ 0\ 1)$ planes of the hexagonal zincite (ZnO) phase, respectively. The peak at $2\theta = 34.6$, which corresponds to the diffraction from the $(0\ 0\ 2)$ plane, is the strongest.

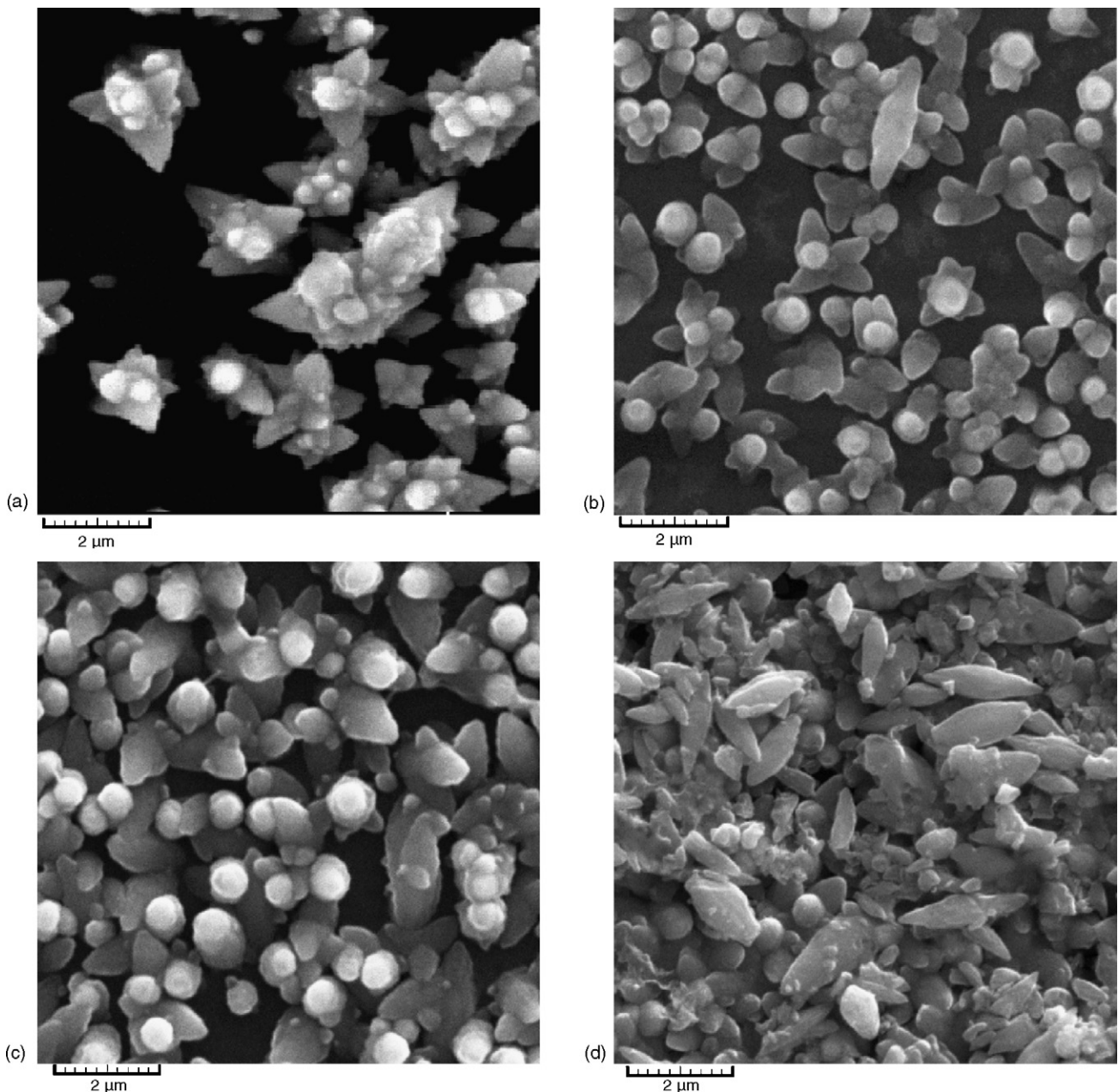


Fig. 7. SEM micrograph of the surfaces of oxide films produced after 100 times of dipping in water at (a) 75 °C, (b) 90 °C, (c) 95 °C, (d) 100 °C.

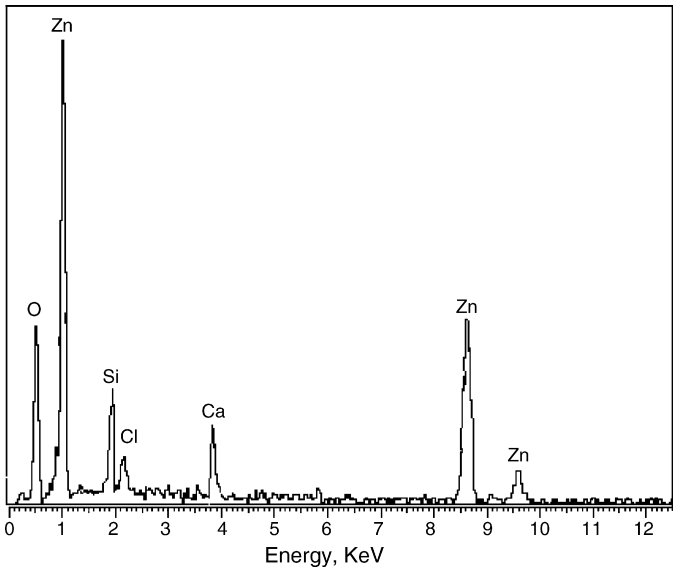


Fig. 8. EDAX elemental analysis of the layer deposited on soda-lime substrate.

The deposited ZnO film showed crystalline character and exhibited a preferential orientation with the *c* axis perpendicular to the substrate. The same preferred orientation has been reported by other investigators who have previously produced ZnO thin films via other methods [23–25]. Other crystals were either non-existent or with negligible appearance on the XRD diffractograms obtained in this research.

Below 10 submerging cycles, the thickness of the film was in the nano range. A smaller crystallite size is a characteristically better layer for gas sensitivity applications. The thickness of the film produced after 40 cycles of the dipping–growing process was, for example, estimated by mass/thickness method to be 1.72 μm . This value was verified by further SEM measurements. Average crystallite size of the grains was determined by Sherrer formulation [26] against number of the dipping–growing cycles. The average size of the crystallites produced after 25 times dipping–growing process was 31.2 nm; after 50 times dipping–growing process, it was 85.5 nm and after 150 times dipping–growing process, it was 225.6 nm; all indicating our good controllability on film thickness and crystallites sizes.

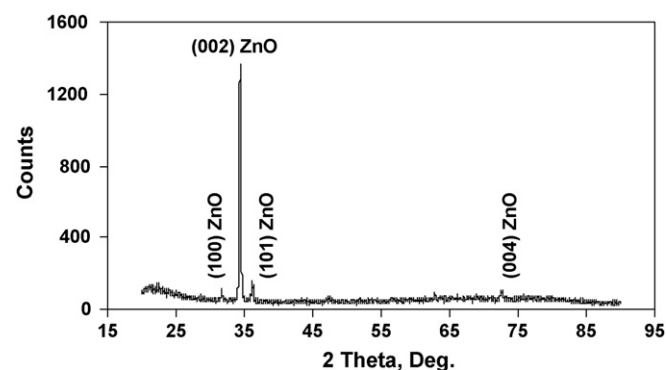


Fig. 9. The diffractogram of the oxide film produced after 40 times dipping–growing process.

4. Conclusions

Pure ZnO thin films can easily be deposited by successive immersion of soda-lime substrate into a cold ammonia complex containing solution and then into hot water. Varying the number of successive dipping–growing stages, one can control the thickness of the film. Film thicknesses are linearly proportional to the number of the dipping–growing cycles. With dipping numbers lower than 9, the film thickness can lie on the nano range. At larger numbers, thicker films are produced. The average size of the crystallites determined by Sherrer equation and verified with SEM measurements indicates a desirable controllability of the crystallite sizes.

Since the proposed method looks both economically and toxically feasible, it can practically be attractive to the industrial design engineer as well as the production managers. For theoretically oriented audience, growth kinetics of the TSCD film is found to follow zeroth order with respect to the concentration and first order with respect to the temperature. XRD results show a polycrystalline thin layer consisting of pure ZnO species at all experimental conditions practically experienced in this research. A combination of the convection heat transfer equation with the diffuse-interface kinetic model gave an overall film growth rate proportional to the difference between the hot water and the substrate temperatures. The overall activation energy and frequency factor of the process was determined to be $17.20 \pm 0.42 \text{ kJ mol}^{-1}$ and $2.81 \pm 0.07 \mu\text{m s}^{-1}$, respectively.

Acknowledgements

The authors would like to thank Mrs. Poupak Amini of X-ray laboratory of Sharif University of Technology for performing the XRD experiments, Mr. Ehsan Jahedizadeh of SEM laboratory of Tehran University for his assistance in preparation of SEM images and the deputy of research of Sharif University of Technology for financial support of the research.

References

- [1] D. Kohl, *J. Phys. D: Appl. Phys.* 34 (19) (2001) R125–R149.
- [2] F. Rosei, *J. Phys. Condens. Matter.* 16 (17) (2004) S1373–S1436.
- [3] J.M. Fini, *Measur. Sci. Technol.* 15 (6) (2004) 1120–1128.
- [4] G. Whitenett, G. Stewart, K. Atherton, B. Culshaw, B. W. Johnstone, *J. Opt. A: Pure Appl. Opt.* 5 (5) (2003) S140–S145.
- [5] C. Bittencourt, E. Liobet, M.A.P. Silva, R. Landers, L. Nieto, K.O. Vicaro, J.E. Sueiras, J. Calderer, X. Correig, *Sens. Actuators B* 92 (2003) 67–72.
- [6] K. Sadrnezhad, *J. Eng.* 1 (1988) 73–78.
- [7] P. Nunes, E. Fortunato, A. Lopes, R. Martins, *Int. J. Inorg. Mater.* 3 (2001) 1129–1131.
- [8] J. Mizsei, J. Voutilainen, S. Saukko, V. Lantto, *Thin Solid Films* 391 (2001) 209–215.
- [9] G. Korotcenkov, V. Macsanov, V. Brinzari, V. Tolstoy, J. Schwank, A. Cornet, J. Morante, *Thin Solid Films* 467 (2004) 209–214.
- [10] J.S. Kim, H.J. Marzouk, P.J. Reecroft Jr., C.E. Hamrin, *Thin Solid Films* 217 (1992) 133–137.
- [11] K. Ramamoorthy, C. Sanjeeviraja, M. Jayachandran, K. Sankaranarayanan, D. Bhattacharaya, L.M. Kukreja, *J. Cryst. Growth* 226 (2001) 281.
- [12] A. Kuroyanagi, *Jpn. J. Appl. Phys.* 28 (1989) 219–222.

- [13] H. Gopaldaswamy, P.J. Reddy, *Semicond. Sci. Technol.* 5 (1990) 980–981.
- [14] A. Tarre, A. Rosental, J. Sundqvist, A. Harsta, T. Unstare, V. Sammelseg, *Surf. Sci.* 532–535 (2003) 514–518.
- [15] O. Shik Kwon, S.-I. Hwang, C.H. Shim, B.C. Kim, G.H. Rue, J.S. Huh, D.D. Lee, *Sens. Actuators B* 89 (2003) 158–163.
- [16] M. Ristova, G.J. Sinadinovski, I. Grozdanov, M. Mitreski, *Thin Solid Films* 149 (1987) 65–71.
- [17] N. Jayadev, S.N. Sainkar, R.N. Karekar, R.C. Aiyer, *Thin Solid Films* 325 (1998) 254–258.
- [18] S.K. Sadmezhaad, *Kinetics Processes in Materials Engineering and Metallurgy*, 2nd ed., Amir Kabir Pub. Inst., Tehran, Iran, 2004 (in Persian).
- [19] D.P. Norton, Y.W. Heo, M.P. Ivill, K. Ip, S.J. Pearton, M.F. Chisholm, T. Steiner, *Mater. Today* 7 (2004) 34–40.
- [20] M.F. Lengke, R.N. Tempel, *Geochim. Cosmochim. Acta* 65 (2001) 2241–2255.
- [21] A.U. Mane, K. Shalini, A. Wohlfart, A. Devi, S.A. Shivashankar, *J. Cryst. Growth* 240 (2002) 157–163.
- [22] C.E. Franklin, F. Seebacher, *J. Exp. Biol.* 206 (2003) 1143–1151.
- [23] K. Ito, K. Nakamura, *Thin Solid Films* 286 (1996) 35–36.
- [24] M. Ristov, G.J. Sinadinovski, I. Grozdanov, M. Mitreski, *Thin Solid Films* 149 (1987) 65–71.
- [25] S. Woo Lee, P.P. Tsai, H. Chen, *Sens. Actuators B* 67 (2000) 122–127.
- [26] A. Ahmad, J. Walsh, T.A. Wheat, *Sens. Actuators B* 93 (2003) 538–545.